The prediction of residual stress and its influence on the mechanical properties of weld joint

2017 J. Phys.: Conf. Ser. 843 012001

(http://iopscience.iop.org/1742-6596/843/1/012001)

IOP Conf. Series: Journal of Physics: Conf. Series **843** (2017) 012001 doi:10.1088/1742-6596/843/1/012001

The prediction of residual stress and its influence on the mechanical properties of weld joint

J. Ni[1] and M. A. Wahab[1]

[1] Ghent University, Laboratory Soete, Belgium

E-mail: magd.abdelwahab@ugent.be

Abstract. A three-dimensional metallo-thermo-mechanical analysis of bead on plate welding is performed in this work. This coupled model enables to capture the microstructural development and temperature history at local region. As a result, the residual stress is evaluated based on the temperature-dependent mechanical properties computed by the mixture of individual phase. Isotropic hardening is assumed in the finite element (FE) analysis. At the same time, the distribution of residual stress is also predicted by treating the mechanical properties as integral values of sheet metal. The two simulated fields of stress and strain after welding are analysed and compared. Moreover, as it is known that welding changes the mechanical properties of the original material, especially in fusion zone (FZ) and heat affected zone (HAZ), the stress and strain data at interested areas (HAZ and FZ) are subtracted for comparison. The predicted stress and strain fields are imported to subsequent simulation of standard tensile test. The stress-strain curves are compared with the one of base material. It is found that residual stress has significant influence on the structural performance of weld joints.

1. Introduction

Residual stress in welded structure or component can result in increasing degradation of mechanical performance. In existence of residual stress, the corrosion is accelerated and fatigue cycle is shortened [1]. Therefore, understanding the generation of residual stress and predicting its distribution are of the utmost importance for welding process.

The welding simulation is always performed in finite element (FE) code as an efficient tool for prediction of residual stress and strain [2-4]. However, some of the researchers [3, 5] simply treated the steel as an overall material and adopted temperature-dependent properties of specific steel for simulation. Other authors [2, 6] included the effect of phase transformation in analysis but only the main product martensite is evaluated. To predict residual stress in a more reasonable way, the development of all transformation products need to be tracked [7]. The most common metallurgical model is the Johnson-Mehl-Avrami-Kolmogorov (JMAK) equation [8], which describes the isothermal transition and is often implemented with the additivity law [9-11] for anisothermal process. One flexible model is proposed by Leblond et al. [12] in which the volume fraction is expressed in an incremental function of equilibrium volume fraction and characteristic time. The function is capable of predicting microstructural development in arbitrary thermal history. Although widely used, parameters in both models need to be calibrated with time-temperature-transformation (TTT) and/or continuous cooling transformation (CCT) diagrams. Differently, Bhadeshia et al. [13-16] published a series of research

works which amount to a metallurgical model that is independent of metallurgical diagrams. In the present work, the model of Bhadeshia et al. [13-16] is chosen to track the microstructural evolution.

As the microstructure is determined, the expansion coefficient, elastic modulus, Poisson's ratio and yield stress are interpolated linearly according to the volume proportion. Two plastic models, i. e. perfectly plastic and linear hardening, are performed. To analyze the effect of phase transformation, simulation which treats the material as an overall unit is also conducted. The resultant residual stress of all the three simulations and the distribution of product phases are extracted and presented for comparison. Finally, the residual stress is imported to another model to conduct tensile test simulation.

2. Experimental setup

Bead-on-plate specimen is manufactured from low-alloyed sheet metal S700 by Gas Metal Arc Welding (GMAW). The thickness of the plate is 8.0 mm and the length 800 mm. Although the metallurgical model is independent of continuous cooling transformation (CCT) diagram, the chemical compositions of plate and filler material (FM) are needed, which are listed in Table 1. The welding speed is controlled at 300 mm/min so that continuous bead is obtained.

Table 1. Chemical composition of S700 and filler material

	Main alloying elements (wt.%)			
	C	Si	Mn	Ni + Mo + Cr
Plate	0.06	0.05	1.9	0.7
FM	0.1	0.9	1.5	

3. Finite element analysis

Finite element analysis (FEA) should be well conducted and may require experiences and skills. FEA has been widely used in the literature for many engineering applications that have been recently published [17-34]. The commercial FE code ABAQUS is used to conduct the coupled thermo-metallo-mechanical analysis. Figure 1 shows the bead geometry after welding predicted by another commercial software. It is seen that the resultant bead geometry is not symmetric. Therefore, the whole dimension model rather symmetric model is built for simulation.

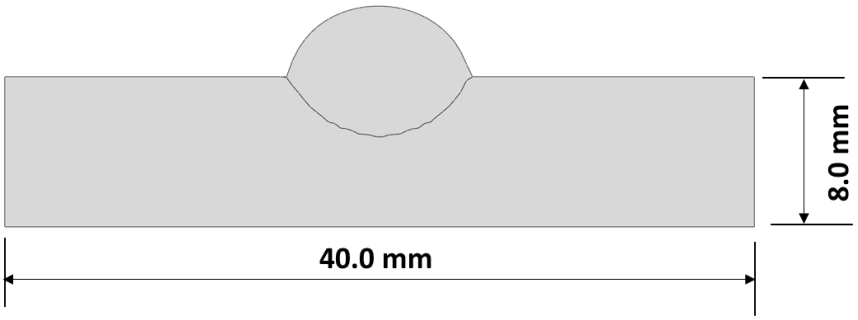

Figure 1. Geometry of the cross-section of bead-on-plate

An approximated heat source proposed by Goldak et. al. [35] is used to simulate the development of temperature field during the whole process. The power distribution q in front quadrant is expressed as [35]:

$$q(x,y,z,t) = \frac{6\sqrt{3}f_f Q_{inp}}{a_f bc\pi\sqrt{\pi}} e^{-3[x+v(\tau-t)]^2/{a_f}^2} e^{-3y^2/b^2} e^{-3z^2/c^2} \quad (1)$$

The fraction of front ellipsoid is denoted by f_f. Parameters a_f, b and c are the lengths of ellipsoid semi-axes. Q_{inp} is heat input rate, v is the welding speed and τ a lag factor needed to define the position of the heat source at $t = 0$. The distribution in rear quadrant is written in the same way, but with different fraction f_r and semi-axis a_r. The calibrated parameters are listed in Table 2. The heat source is applied in ABAQUS by writing user subroutine DFLUX.

Table 2. Calibrated parameters in heat source

a_f (mm)	a_r (mm)	b (mm)	c (mm)	f_f	Q_{inp} (W)
7.0	19.5	4.8	3.2	1.5	5474

Moreover, the temperature-dependent thermal properties are used in order to precisely capture the temperature. The value of the specific heat ($\boldsymbol{c}$) and heat conductivity ($\boldsymbol{k}$) are shown in Figure 2. The thermal properties at 1400°C will be used for situation where temperature exceeds 1400°C.

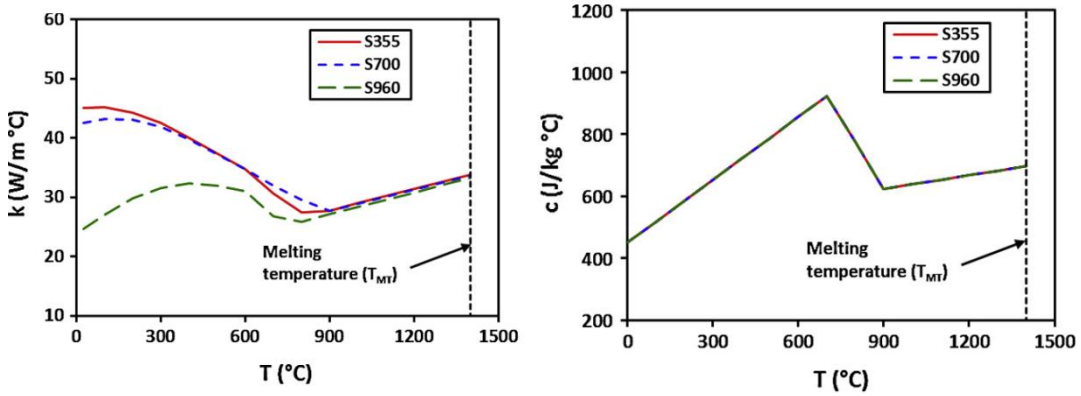

Figure 2. Temperature dependent thermal properties $\boldsymbol{c}$ and $\boldsymbol{k}$ [3]

To analyze the influence of microstructure, the volume fractions of each phase or micro-constituent are predicted by the metallurgical framework of Bhadeshia [13-16]. In his model, the start and finish transformation temperatures are estimated based on thermodynamic theories rather than empirical function. For transforming kinetics, the model assumes the reconstructive transformation to occur at grain boundaries but also includes the possibility of inclusion nucleation. The nucleation rates were treated as temperature-dependent and the growth rates were determined by solving carbon diffusion equations [13]. The initiation of bainite growth was assumed to be displacive with a strain energy of 400 J/mol [36]. The advantages of this framework are: 1) it omits the necessity of determining parameters with known results and 2) it requires only the basic information of the chemical composition, the temperature history and the austenite grain size for input. Totally, five products, allotriomorphic ferrite (α), Widmannstätten ferrite (α_w), pearlite (α_p), bainite (α_b) and martensite (α') are considered in the simulation. The sequence in which the individual phase is arranged is listed in Table 3.

Table 3. The sequence of field variables and corresponding phase

FV1	FV2	FV3	FV4	FV5	FV6
α	α_w	α_p	α_b	α'	γ

The material property are assigned in two ways. As the base material and the beam are treated as single unit, the whole model is applied unique temperature-dependent mechanical properties, which are shown in Figure 3. The Poisson's ratio is considered to be constant value of 0.29 over whole temperature range.

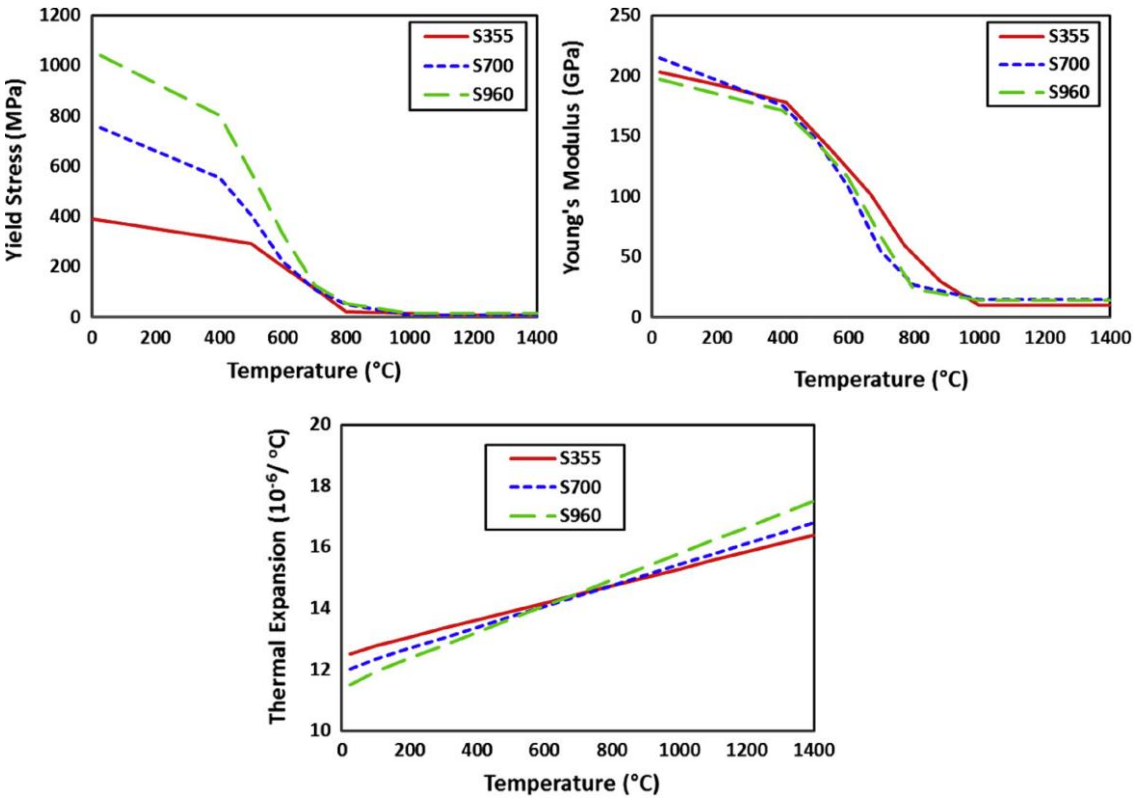

Figure 3. Temperature dependent yield stress, Young's modulus and thermal expansion [3]

The second method, which treats the material as an assembly of phases or constituents, applies mechanical properties to individual microstructure. The mechanical properties are listed in Table 4. The overall mechanical properties are obtained by linearly interpolating the individual properties with corresponding volume fractions. The property of α_W is not listed in Table 4 but it is considered the same as α and α_p. With interpolation, two hardening cases, i. e. perfectly plastic and isotropic hardening (the tangent modulus of which is assumed to be 2000 MPa) are simulated.

Table 4. The sequence of field variables and corresponding phase [37]

		Temperature (°C)			
Property	Phase	0	300	600	800
Elastic modulus, GPa	γ	200	175	150	124
	α and α_p	210	193	165	120
	α_b	210	193	165	120
	α'	200	185	168	--
Poisson's ratio	γ	0.29	0.31	0.33	0.35
	α and α_p	0.28	0.30	0.31	0.33
	α_b	0.28	0.30	0.31	0.33
	α'	0.28	0.30	0.31	--

Expansion coefficient, K^{-1}	γ		2.1×10^{-5}		
	α and α_p		1.4×10^{-5}		
	α_b		1.4×10^{-5}		
	α'		1.3×10^{-5}		
Yield strength, MPa	γ	190	110	30	20
	α and α_p	360	230	140	30
	α_b	440	330	140	30
	α'	1600	1480	1260	--

The main algorithm is summarized in Figure 4. The thermal analysis is run before metallurgical and mechanical analyses in order to calculate the cooling rate. Therefore, the proposed model is sequential coupled, which ignores the effects of latent heat and plastic work. However, it is reasonable since the amount of energy produced by these two terms is far less than the welding power [38, 39]. The initial temperature of the whole structure is assigned to 20°C and the convection coefficient is $30W/m^2°C$.

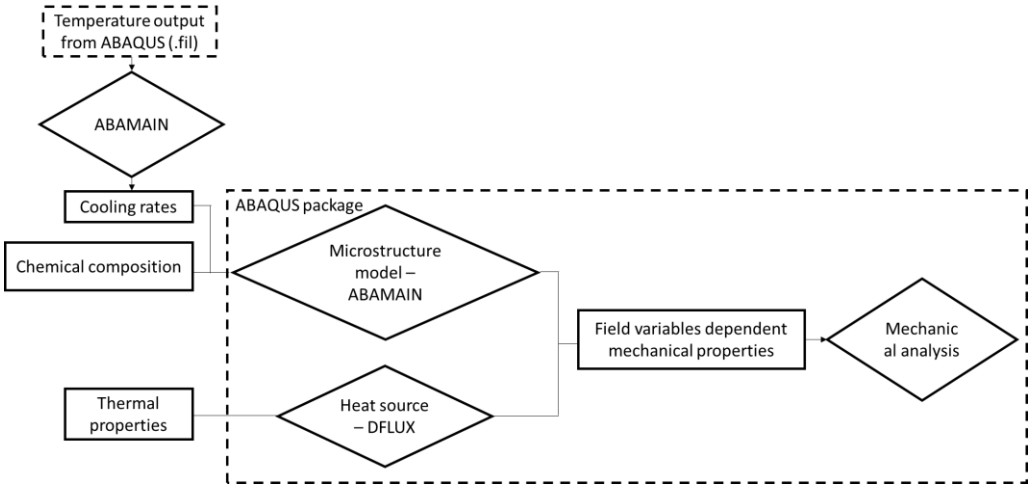

Figure 4. Flow chart of the fully coupled model

After the simulation of welding process, the structure is further subjected to a tensile load along the welding direction. The stress and strain curves are plotted in different region to show the influence of residual stress on mechanical performance of weld structure.

4. Results and discussion

The temperature histories of two nodes, A and B as shown in Figure 5, are plotted. Node A is selected inside melt region and Node B lies at the boundary between FZ and HAZ. It is seen that the maximum temperature that Node B experiences is about 1400°C, which is in agreement with the experimental data [3]. This accordance shows the reasonability of the calibrated heat source model. The distribution of α_W (Widmannstätten ferrite) at the end of simulation is also presented. Since the temperature at A drops faster than B and the transformation to α_W is displacive, the volume fraction of α_W at A should be higher than the value at B. This conclusion is validated by the contour plot of FV2 in Figure 5.

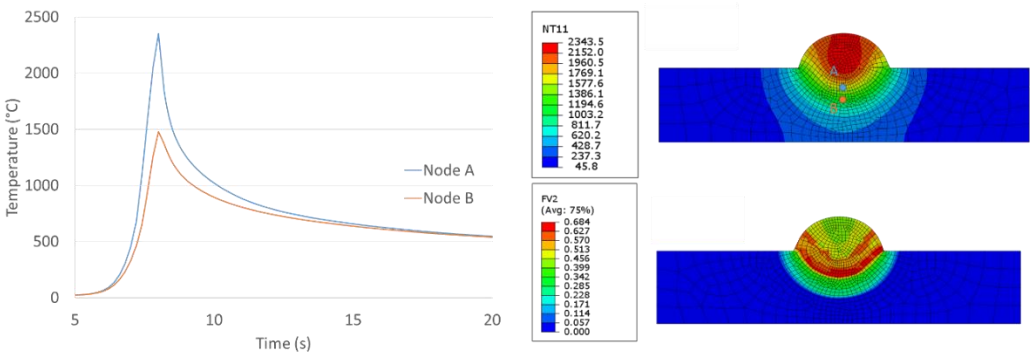

Figure 5. Temperature histories of nodes and contour plots of temperature and α_W

As it is mentioned in section 3. three different approaches are used to apply mechanical properties. The first approach is to interpolate the values corresponding to phase volume fraction at various temperature and assumes a linear hardening tangent modulus of 2000 MPa (IPLH). The second way interpolates the mechanical properties similarly but assumes perfectly plastic (IPPP). The third approach simply uses overall mechanical properties as shown in Figure 3 and assumes perfectly plastic as well (OPPH).

The transverse residual stress at the plate surface of middle section is presented in Figure 6. In all three cases, the transverse residual stress is tensile. This is reasonable since as the weld cools down, the material of this region begins to shrink. However, the tensile stress is not equally distributed. It increases at first as it approaches to the centreline and drops to minimum value at the boundary between HAZ and FZ. All the three simulation results share the same distribution pattern. The peak value of transverse stress in linear hardening case is highest among the three analysis, which means that the tensile stress caused by cooling is large enough to yield the material. When the material is assumed to be perfectly plastic, the transverse stress in FZ calculated by interpolating properties is lower than using overall properties. In this region, the stress state is not sufficient to cause a global yield and as a result, the influence of individual phase becomes clear. Since α_W and α' possess higher specific volume than γ, the transition from γ to α_W and α' will lead to an extra expansion. This expansion releases the tensile stress partially, which explains the lower value of transverse stress when using interpolated properties.

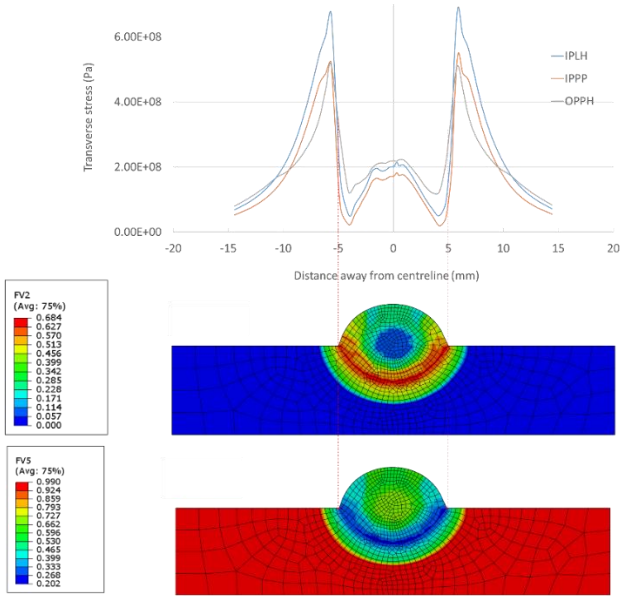

Figure 6. Transverse residual stress at middle cross section and volume fractions of α_W and α'

Finally, a homogenous load is applied to the welded structure in longitudinal direction (or welding direction). The stress-strain curves are plotted at three positions, A, B and C. It can be seen that in existence of residual stress (A and B), the relation between stress and strain is no longer linear. The bead is subjected to tensile stress in longitudinal direction in initial, which leads to a faster yielding. In contrast, the material in HAZ is subjected to compressive state.

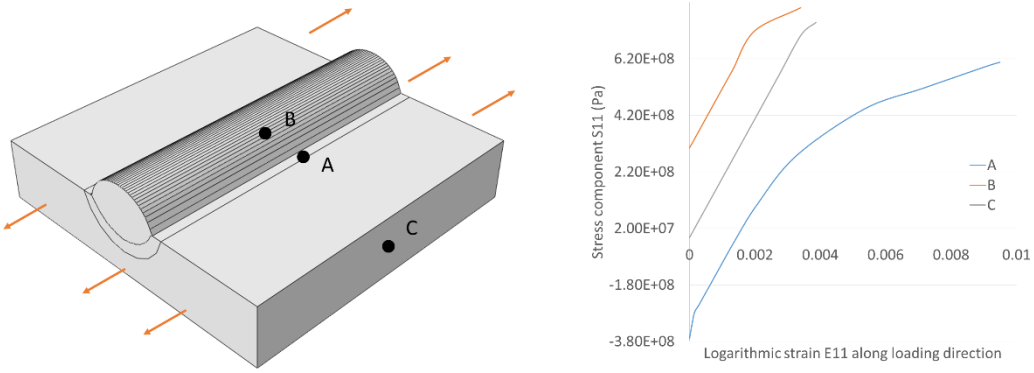

Figure 7. The stress-strain curves of selected points

5. Conclusion

A fully coupled thermo-metallo-mechanical model is developed to predict the distribution of residual stress and analyse its influence on mechanical behaviour. The metallurgical model proposed by Bhadeshia et al. [13-16] proves an efficient way to track the microstructural development. To evaluate the influence of phase transformation on residual stress, mechanical properties are interpolated with the phase volume fraction. By comparing with the result from an overall model, it is found that the volume expansion due to transition will affect the magnitude and distribution of residual stress, especially in FZ. In the zone where material is already yielded, the difference of residual stress is not so significant. Moreover, a tensile test simulation is performed subsequently after the welding simulation. The stress-strain curves of three typical regions show that the material in FZ and HAZ does not behaves linearly even in elastic region. As the welded structure is subjected to external load, the residual stress will accelerate yielding in some areas while retard yielding in other areas, which makes the prediction of structure failure even more complicated.

6. Acknowledgements

The authors would like to acknowledge the MaDurOS project and the support from SIM and VLAIO.

7. References

[1] Barsoum Z and Barsoum I 2009 *Engineering Failure Analysis* **16**(1) 449-467
[2] Deng D and Murakawa H 2008 *Computational Materials Science* **43**(4) 681-695
[3] Bhatti AA, Barsoum Z, Murakawa H and Barsoum I 2015 *Materials & Design* **65** 878-889
[4] Junyan Ni and Wahab MA 2017 *Computers & Structures* **186** 35–49
[5] Teng TL and Lin CC 1998 *International Journal of Pressure Vessels and Piping* **75**(12) 857-864
[6] Deng D 2009 *Materials & Design* **30**(2) 359-366
[7] Borjesson L and Lindgren LE 2001 *Journal of Engineering Materials and Technology-Transactions of the Asme* **123**(1) 106-111
[8] Avrami M 1939 *The Journal of Chemical Physics* **7**(12) 1103-1112
[9] Cahn JW 1956 *Acta Metallurgica* **4**(6) 572-575

[10] Deng D, Ma N and Murakawa H 2012 *Transactions of JWRI* **2011** 79-82
[11] Inoue T 1996 *Transactions of JWRI* **25**(2) 69-87
[12] Leblond JB and Devaux J 1984 *Acta Metallurgica* **32**(1) 137-146
[13] Jones SJ and Bhadeshia HKDH 1997 *Acta Materialia* **45**(7) 2911-2920
[14] Takahashi M and Bhadeshia HKDH 1991 *Materials Transactions Jim* **32**(8) 689-696
[15] Khan SA and Bhadeshia HKDH 1990 *Materials Science and Engineering a-Structural Materials Properties Microstructure and Processing* **129**(2) 257-272
[16] Rees GI and Bhadeshia HKDH 1992 *Materials Science and Technology* **8**(11) 985-993
[17] X. Nguyen H, N. Nguyen T, Abdel Wahab M, Bordas SPA, Nguyen-Xuan H and P. Voa T 2017 *Computer Methods in Applied Mechanics and Engineering* **313** 904-940
[18] Tran Vinh L, Lee J, Nguyen-Van H, Nguyen-Xuan H and Abdel Wahab M 2015 *International Journal of Non-Linear Mechanics* **72** 42-52
[19] Tran LV, Phung-Van P, Lee J, Wahab MA and Nguyen-Xuan H 2016 *Composite Structures* **140** 655-667
[20] Thai CH, Ferreira AJM, Abdel Wahab M and Nguyen-Xuan H 2016 *Acta Mechanica* **227**(5) 1225-1250
[21] Thai C, Zenkour AM, Abdel Wahab M and Nguyen-Xuan H 2016 *Composite Structures* **139** 77-95
[22] Phung-Van P, Tran LV, Ferreira AJM, Nguyen-Xuan H and Abdel-Wahab M 2016 *Nonlinear Dynamics* 1-16; doi:10.1007/s11071-11016-13085-11076
[23] Phung Van P, Nguyen LB, Tran Vinh L, Dinh TD, Thai CH, Bordas SPA, Abdel Wahab M and Nguyen-Xuan H 2015 *International Journal of Non-Linear Mechanics* **76** 190-202
[24] Phung Van P, De Lorenzis L, Thai CH, Abdel Wahab M and Nguyen-Xuan H 2015 *Computational Materials Science* **96** 495-505
[25] Phung Van P, Abdel Wahab M, Liew KM, Bordas SPA and Nguyen-Xuan H 2015 *Composite Structures* **123** 137-149
[26] Yue T and Abdel Wahab M 2017 *Tribology International* **107** 274-282
[27] Yue T and Abdel Wahab M 2016 *Materials* **9** 597; doi:510.3390/ma9070597
[28] Resende Pereira KdF, Bordas S, Tomar S, Trobec R, Depolli M, Kosec G and Abdel Wahab M 2016 *Materials* **9** 639; doi:610.3390/ma9080639
[29] Noda N-A, Chen X, Sano Y, Wahab MA, Maruyama H, Fujisawa R and Takase Y 2016 *MATERIALS & DESIGN* **96** 476-489
[30] Ferjaoui A, Yue T, Abdel Wahab M and Hojjati-Talemi R 2015 *International Journal of Fatigue* **73** 66-76
[31] Tran Vinh L, Lee J, Ly HA, Abdel Wahab M and Nguyen-Xuan H 2015 *International Journal of Mechanical Sciences* **96-97** 65-78
[32] Yue T and Abdel Wahab M 2016 *Materials* **9**(7)
[33] Phung-Van P, Qui LX, Nguyen-Xuan H and Wahab MA 2017 *Composite Structures* **166** 120–135
[34] Phung-Van P, Ferreira AJM, Nguyen-Xuan H and Abdel Wahab M 2017 *Composites Part B: Engineering* **118** 125-134
[35] Goldak JA and Akhlaghi M 2006 Computational welding mechanics ed editors. Springer Science & Business Media
[36] Bhadeshia HKDH 1981 *Acta Metallurgica* **29**(6) 1117-1130
[37] Totten GE 2002 Handbook of Residual Stress and Deformation of Steel ed editors. ASM International
[38] Kirkaldy JS and Sharma RC 1982 *Scripta Metallurgica* **16**(10) 1193-1198
[39] Dai H 2012 Modelling residual stress and phase transformations in steel welds ed editors. INTECH Open Access Publisher